Pravastatin Attenuates Carboplatin-Induced Nephrotoxicity in Rodents via Peroxisome Proliferator-Activated Receptor Alpha–Regulated Heme Oxygenase-1

Hsi-Hsien Chen, Tzen-Wen Chen, Heng Lin

Graduate Institute of Clinical Medicine, College of Medicine, Taipei Medical University, Taipei, Taiwan (H-H.C., T-W.C); Department of Internal Medicine, Taipei Medical University Hospital, Taipei, Taiwan (H-H.C., T-W.C); Graduate Institute of Pharmacology and Toxicology, Tzu Chi University, Hualien, Taiwan (H.L.)

1

Running title: Pravastatin-Induced Decrease in Carboplatin Nephrotoxicity

Address correspondence to: Heng Lin, Graduate Institute of Pharmacology and Toxicology,

Tzu Chi University, No.701 Zhongyang Rd., Sec. 3, Hualien, 97004 Taiwan; Phone:

886-02-27899135; Fax: 886-02-27827654; e-mail address: linheng@ibms.sinica.edu.tw.

Number of text pages: 35 total manuscript pages/21 main text pages

Number of figures: 7 (plus 6 supplemental figures)

Number of tables: 0

Number of references: 30

Abstract: 198

Introduction: 531

Discussion: 1510

Nonstandard abbreviations: ChIP, chromatin immunoprecipitation; CM-H$_2$DCFDA,

chloromethyl-2',7'-dichlorodihydrofluorescein diacetate; COX-2, cyclooxygenase-2; DCF,

dichlorodihydrofluorescein; HMG-CoA, 3-hydroxy-3-methylglutaryl-coenzyme A; HO-1,

heme oxygenase-1; IL, interleukin; NO, nitric oxide; PGI$_2$, prostaglandin I$_2$; PPARα,

peroxisome proliferator-activated receptor-α; PPRE, peroxisome proliferator response

element; ROS, reactive oxygen species; siRNA, small interfering RNA; TUNEL, terminal

deoxynucleotidyl transferase dUTP nick end labeling.

ABSTRACT

The aim of this study was to explore the molecular mechanisms underlying the protective effect of pravastatin against carboplatin-induced nephrotoxicity in rodents. We exposed rat NRK-52E renal tubular epithelial cells to carboplatin, with or without pravastatin. Pravastatin decreased production of reactive oxygen species (ROS), increased expression of heme oxygenase-1 (HO-1), cyclooxygenase-2 (COX-2), and 6-keto prostaglandin (PG) F1α, enhanced nuclear translocation of peroxisome proliferator-activated receptor-α (PPARα), and increased HO-1 promoter and peroxisome proliferator response element (PPRE) activities. We found interaction of PPARα with PPRE on the HO-1 promoter in nuclear extracts from pravastatin-treated NRK-52E cells and by chromatin immunoprecipitation. We pretreated mice with pravastatin and then administered a single intraperitoneal injection of carboplatin. Effects on renal function, morphology, apoptosis, and survival were assessed. In response to carboplatin injection, mice developed acute renal failure, with elevated activated caspase-3, increased apoptotic bodies, and decreased survival. Pretreatment with pravastatin significantly ameliorated renal dysfunction and apoptosis and improved renal morphology and survival. Injection of pravastatin also induced overexpression of PPARα and HO-1 in wild-type mice, and HO-1 expression was significantly attenuated in PPARα-knockout mice. These results indicate that pravastatin upregulates HO-1 and protects against carboplatin-induced renal dysfunction and apoptosis via a PPARα-dependent pathway.

Carboplatin (cis-diammine-1,1-cyclobutane dicarboxylate platinum II), a second-generation, platinum-containing, anticancer drug, is currently used in the treatment of lung and ovarian cancers, as well as head and neck cancers (Fujiwara et al., 2003; Pivot et al., 2001). Because carboplatin has fewer toxic effects than cisplatin, it can be used at higher doses to achieve optimal antitumor effects (reviewed by Alberts, 1995). However, its byproduct, platinum-ammine-DNA adduct, accumulates in the kidney and induces renal tubular damage (reviewed by Kintzel, 2001); this limits its use.

3-Hydroxy-3-methylglutaryl-coenzyme A (HMG-CoA) reductase inhibitors (statins) are lipid-lowering agents that are widely used in medical practice to lower plasma levels of low-density lipoprotein cholesterol. It is generally accepted that mechanisms beyond the reduction of plasma cholesterol contribute significantly to the anti-atherogenic and tissue-protective properties of statins (reviewed by Takemoto and Liao, 2001). Cholesterol-independent effects of statins include indirect anti-inflammatory effects such as activation of reduction-oxidation reaction (redox)–sensitive transcription factors (Gueler et al., 2002). Statins also protect tissues from various types of insults such as ischemia-reperfusion injury in the kidney and heart (Gueler et al., 2007; Birnbaum et al., 2005; Li, Yang et al., 2004; Cheng et al., 2008).

Some studies have demonstrated that statins lead to activation of the promoter for the antioxidant defense protein heme oxygenase-1 (HO-1), along with its transcription and

accumulation (Lee et al., 2004), which may help to explain the pleiotropic antioxidant and

anti-inflammatory actions of statins (Grosser et al., 2004). Heme oxygenase-1, an inducible

enzyme that catabolizes heme to biliverdin, ferrous iron, and carbon monoxide, exhibits

cytoprotective effects against oxidative insults (reviewed by Sikorski et al., 2004). There are

many HO-1 inducers including ultraviolet A radiation; hydrogen peroxide; cytokines

(interleukin [IL]-1, IL-6, IL-10, tumor necrosis factor, interferon-γ); endotoxin; growth

factors (platelet-derived growth factor, transforming growth factor-β); oxidized lipids;

hyperoxia; nitric oxide (NO); NO donors; prostacyclin; peroxisome proliferator-activated

receptor (PPAR) α and γ; angiotensin II; and glucose deprivation (reviewed by Ferrándiz and

Devesa, 2008). Several of these stimuli play important roles in the pathophysiology of acute

renal failure (Nath et al., 2001). Heme oxygenase-1 has been shown to be upregulated and to

ameliorate the severity of renal damage in a variety of kidney injury models, such as kidney

transplant rejection (Cuturi et al., 1999), and to inhibit the effects of nephrotoxins induced by

cisplatin and cyclosporine (Agarwal et al., 1995; Li, Wu, et al., 2004).

Peroxisome proliferator-activated receptors are nuclear hormone receptors that form

heterodimers with retinoid X receptors, which then activate or repress target genes. Li, Wu,

and colleagues (2004) reported that pretreatment with Wy-14643, a ligand for PPARα,

ameliorates cisplatin-induced acute renal failure on the basis of changes in blood urea

nitrogen, creatinine, and tissue histology.

Whether statins can protect against carboplatin-induced renal injury via cholesterol-independent pathways is not clear. The effects of statins on PPARα are not completely defined, although another lipid-lowering agent, clofibrate, has been shown to be a ligand for PPARα (Forman et al., 1997). We hypothesized that the protective effects of statins against carboplatin-induced renal injury may be mediated by PPARα and HO-1. To test this hypothesis, we investigated the effects of pravastatin on PPARα and HO-1 in a rat renal epithelial cell line and in mouse models.

Materials and Methods

Animals and treatment with carboplatin and pravastatin. Male C57/B6, H129 wild-type, and H129 PPARα-knockout (PPARα$^{-/-}$) mice received humane care in compliance with the *Principles of Laboratory Animal Care* formulated by the National Society for Medical Research and the *Guide for the Care and Use of Laboratory Animals* prepared by the Institute of Laboratory Animal Resources (National Institutes of Health publication No. 86-23, revised 1985). The study protocol was approved by our institutional ethics committee on animal research. Pravastatin (Sigma-Aldrich, St. Louis, MO) was dissolved in double-distilled water, and carboplatin (Sigma-Aldrich) was dissolved in dimethyl sulfoxide (DMSO) just before use.

Ten-week-old mice were administered an intraperitoneal (i.p.) injection of a single

dose of carboplatin (100 mg/kg), with (experimental group) or without (control group) i.p.

injection with pravastatin (5 mg/kg) (Sigma-Aldrich) 1 day before carboplatin treatment. The

control group was treated with the same volume of normal saline (i.p.) instead of pravastatin.

Cell culture and transfection. The NRK-52E renal tubule epithelial cell line was

obtained from American Type Culture Collection (ATCC, Manassas, VA) and cultured in

Dulbecco modified Eagle medium supplemented with 10% fetal bovine serum, 100 units/ml

penicillin, and 100 μg/ml streptomycin at 37°C in an atmosphere containing 5% CO_2, as

described previously (Chen et al., 2009). Cells were transfected the following day with

Lipofectamine (Invitrogen, Carlsbad, CA) containing 1.5 μg luciferase reporter plasmid and

various amounts of PPARα, PPARα small interfering (si) RNA

(5'CCCTTATCTGAAGAATTCTTA3'), or FLAG-PPARα expression vector per 6-cm^2

culture dish. The amount of DNA was kept constant with the use of empty expression vector.

Cells were subjected to assays 16 to 24 h later.

Measurement of biochemical parameters and extraction of cytoplasmic and

nuclear protein. Blood samples (500 μl) were collected from the tail vein. Samples were

centrifuged (6000 $g \times 3$ min) to separate the serum from the cells. Serum biochemical

parameters were measured within 24 h of blood sampling.

For cytoplasmic and nuclear protein extraction, cells and kidney tissues were separated

into nuclear and cytoplasmic fractions and extracted according to the manufacturer's protocol

(Pierce Chemical Company, Rockford, IL).

Terminal deoxynucleotidyl transferase dUTP nick end labeling. We detected DNA fragmentation in cells and animal tissues by labeling the termini of nucleic acids with the terminal deoxynucleotidyl transferase dUTP nick end labeling (TUNEL) method (Roche, Mannheim, Germany). Mice were perfused with 4% paraformaldehyde in 0.1 M phosphate buffer (pH 7.4). Organs were dissected, postfixed overnight in 4% paraformaldehyde, embedded in paraffin, and sectioned (5-μm thickness). The TUNEL assay was performed according to the manufacturer's protocol.

Nuclear extracts and electrophoretic mobility shift assays. For the peroxisome proliferator response element (PPRE) primer, we designed a PPARα DNA-binding sequence (5'-GAGTTGTAAGGTCATGGGAAA-3') for use in electrophoretic mobility shift assays. Electrophoretic mobility shift assay analysis of nuclear extracts was carried out as described previously (Lin et al., 2008). Binding reactions were performed in 20-μl reaction mixtures with 3 μg of nuclear extract in a buffer containing 12 mM HEPES (pH 7.9), 5 mM MgCl$_2$, 60 mM KCl, 4 mM Tris-HCl (pH 7.9), 0.6 mM ethylenediaminetetraacetic acid (EDTA), 0.6 mM dithiothreitol, 0.5 mg/ml bovine serum albumin, 1 μg poly[d(I-C)], 12% glycerol, and 20,000 cpm radiolabeled, double-stranded, 21-bp PPRE probe for 20 min at room temperature. Reactions were loaded onto a 4% polyacrylamide gel and run at 200 V at room temperature in 0.25× Tris/borate/EDTA buffer. The gel was dried and exposed to x-ray film

(Kodak, Rochester, NY).

Histopathologic preparations and immunocytochemistry. Kidneys from all of the

treated groups were fixed in 10% buffered formalin overnight at 4°C and processed in

paraffin wax. Sections (5-μm thickness) were stained with hematoxylin and eosin.

For immunocytochemistry, NRK-52E cells transfected with FLAG-PPARα plasmid

were plated onto 35-mm poly-L-lysine–coated glass-bottomed dishes (Matsunami Glass Ind.,

Ltd., Osaka, Japan) and fixed for 20 min at room temperature in 4% paraformaldehyde and

0.4% Triton X-100 in phosphate-buffered saline (PBS). The cells were incubated with

antibodies against FLAG (rabbit polyclonal; Sigma-Aldrich) in PBS containing 0.05% Tween

20 (PBST) plus 2% horse serum. After washing three times with PBS, the cells were

incubated with Alexa 488-conjugated anti-rabbit IgG (Molecular Probes, Eugene, OR) and

Cy3-conjugated anti-mouse IgG (Amersham Biosciences, Piscataway, NJ) in PBST

containing 2% horse serum for 1 h at room temperature. Images were obtained with a

fluorescence microscope.

Chromatin immunoprecipitation assay. NRK-52E cells were transfected with

FLAG-PPARα plasmid 1 day after treatment with pravastatin, fixed in 1% formaldehyde, and

chromatin immunoprecipitation (ChIP) assays were performed according to the

manufacture's protocol (Millipore, Billerica, MA). Chromatin was immunoprecipitated with

anti-FLAG antibody (Sigma-Aldrich) and anti-acetyl H4 antibody (Millipore). Purified DNA

9

was detected by standard polymerase chain reaction.

HO-1 promoter and PPRE reporter assay. The human HO-1-α promoter

(positions –800 to +17) and three repeats of the PPRE-binding sequence were each cloned

into pGL2-basic promoterless plasmid vectors (Promega, Madison, WI) and transfected into

NRK-52E cells. Promoter-induced luciferase activity was measured as described previously

(Chen et al., 2009).

Dichlorofluorescein assay for reactive oxygen species. The intracellular formation of

reactive oxygen species (ROS) was detected with the fluorescent probe 5- (and 6-)

chloromethyl-2',7'-dichlorodihydrofluorescein diacetate (CM-H_2DCFDA; Molecular Probes).

NRK-52E cells (10^6 cells/ml) were cultured in the presence of 100 μM carboplatin for 24 h or

pretreated for 30 min with 50 μM pravastatin and then loaded with 0.1 μg/ml CM-H_2DCFDA

at 37°C for 30 min in the dark. Cells were then washed twice with Hank balanced salt

solution (HBSS) containing calcium and magnesium. Dichlorodihydrofluorescein (DCF)

fluorescence was measured immediately with a charge-couple device (CCD) camera (DP72,

Olympus, Melville, NY) coupled to a microscope system (BX51, Olympus) at 100×

magnification.

Statistical analysis. Continuous variables were compared by one-way analysis of

variance (ANOVA). When there was a significant difference between groups, multiple

comparisons of means were performed with the Bonferroni procedure and type-I error

adjustment. All statistical assessments were two-sided and evaluated at the 0.05 level of

significance. Statistical analyses were performed with SPSS 15.0 statistics software (SPSS

Inc., Chicago, IL). Survival analysis was performed according to the Kaplan-Meier method,

and between-group differences in survival were tested by log-rank test.

Results

Carboplatin stimulated apoptosis and caspase activation in vitro and in vivo. To

determine if carboplatin-induced nephrotoxicity occurred via a caspase-dependent pathway in

vitro, NRK-52E renal epithelial cells were treated with increasing carboplatin concentrations

(50–800 μM), which resulted in a concentration-dependent increase in the level of caspase-3

(Fig. 1A); this increase continued for at least 48 h (Fig. 1B). Treatment with the caspase

inhibitor Z-VAD (Merck, Whitehouse Station, NJ) showed that carboplatin induced apoptosis

in a caspase-dependent manner in Western blot and TUNEL assays (Supplemental Figs. 1

and 2). In addition, infection of NRK-52 cells with adenovirus containing HO-1 resulted in

overexpression of HO-1 and a decrease in carboplatin-induced caspase-3 expression

(Supplemental Fig. 3). To assay for possible iron toxicity induced by overexpression of HO-1,

which can result in increased generation of ROS and inflammation, we overexpressed HO-1

by adenovirus infection in neuronal PC-12 cells (Supplemental Fig. 4). Results showed that

overexpression of HO-1 induced ferric iron deposition, which was decreased by treatment

with the iron chelator deferoxamine. We also assayed PC-12 cell cytotoxicity and showed

that overexpression of HO-1 induced more cytotoxicity in PC-12 cells than in NRK-52 cells,

indicating that the effects of HO-1 may be tissue dependent.

We explored the effects of carboplatin in vivo by determining the expression of

caspase-3 in kidney cells of mice injected with 100 mg/kg carboplatin. Immunoblotting

results showed significantly increased staining for caspase-3 in the kidneys of

carboplatin-treated mice (2 days after single treatment; Fig. 1C). Apoptosis in kidney cells of

mice treated with carboplatin was also significantly ($p < 0.01$) increased to 16% compared to

that of control mice (2%) (Fig. 1D).

Pravastatin attenuated carboplatin-induced ROS production, renal cell apoptosis,

and caspase-3 expression. Exposure of NRK-52E renal epithelial cells to 100 μM

carboplatin for 24 h induced production of ROS approximately 25-fold that in saline-treated

cells, as shown by DCF staining (Fig. 2A). This increase in the level of ROS was

significantly ($p < 0.05$) attenuated by pretreatment with 50 μM pravastatin for 30 min.

Pravastatin also significantly ($p < 0.05$) inhibited carboplatin-induced caspase-3 expression in

NRK-52E cells (Fig. 2B). We also performed experiments with cisplatin and showed that this

agent induced caspase-3 expression in NRK-52 cells, which was attenuated by treatment with

pravastatin (Supplemental Fig. 5).

In vivo experiments showed that i.p. injection of mice with pravastatin significantly (p

< 0.01) reduced not only the rate of apoptosis in kidney cells, from 14% to 3% (Fig. 2C), but

also the expression of cleaved, active caspase-3 compared to mice treated with carboplatin

alone ($p < 0.05$) (Fig. 2D).

Pravastatin improved renal function and survival in mice treated with

carboplatin. Carboplatin treatment resulted in abnormal renal function, as revealed by the

levels of serum urea nitrogen and creatinine measured 5 days after injection. This effect was

improved by pretreatment with pravastatin (Fig. 3B). In accordance with these markers of

renal function, control mice and mice treated with pravastatin showed healthy, histologically

comparable tubular systems (Fig. 3Ca, b). However, kidneys of mice treated with carboplatin

showed substantial histopathologic changes such as tubular necrosis and dilation, protein

casts, and loss of brush borders (Fig. 3Cc). Injection with pravastatin in addition to

carboplatin produced marked decreases in these features (Fig. 3Cd).

Survival of mice injected with 100 mg/kg carboplatin was markedly decreased

compared to that of control mice. Treatment with pravastatin in addition to carboplatin

significantly ($p < 0.01$) increased 7-day survival compared to mice treated with carboplatin

alone, as determined by Kaplan-Meier analysis (Fig. 3A).

Pravastatin induction of HO-1 in NRK-52E cells involved cyclooxygenase-2 and a

PPARα pathway. To test whether the renal protective effect of pravastatin was mediated by

HO-1, NRK-52E cells were treated with 20 μM pravastatin for 24 or 48 h, and the expression

of HO-1 was determined by immunoblotting. As shown in Fig. 4A, the expression of HO-1

was increased after treatment with pravastatin for 24 h. However, HO-1 expression decreased

when pravastatin treatment was continued for 48 h.

A similar temporal response was observed when we examined the effect of pravastatin

on the expression of cyclooxygenase (COX)-2. To determine whether overexpression of

COX-2 might increase the intracellular level of 15d-prostaglandin (PG)I$_2$, a ligand for

PPARα, we examined the effect of 20 μM pravastatin on the level of 6-keto PGF1α (the

stable hydrolysis product of PGI$_2$) with an enzyme immunoassay system. As observed for the

expression of COX-2, pravastatin also induced an increase in 6-keto PGF1α at 24 h (Fig. 4B).

Similarly, pravastatin increased the levels of PPARα and HO-1 in NRK-52E cells (Fig. 4C).

We next examined whether inhibition of PPARα and COX-2 affected the expression of

HO-1. When PPARα was inhibited by transfection of pravastatin-treated cells with plasmid

containing PPARα siRNA, the expression of PPARα and HO-1 was reduced (Fig. 4C). When

the COX-2 inhibitor NS-398 (Cayman Chemical, Ann Arbor, MI) was added to

pravastatin-treated cells, the increase in HO-1 was again significantly decreased, and

administration of NS-398 and PPARα siRNA in combination showed a synergistic reduction

in the level of HO-1 (Fig. 4D).

Pravastatin enhanced PPARα nuclear translocation in NRK-52E cells. We next

examined whether pravastatin enhanced nuclear translocation of PPARα. As shown in Fig.

5A, the level of cytosolic PPARα was not significantly affected by pravastatin in NRK-52E

cells transfected with plasmid containing FLAG-PPARα. However, the level of nuclear

PPARα was significantly increased in pravastatin-treated cells (Fig. 5A, lane 3 vs lane 4).

Immunostaining also showed that FLAG-PPARα translocated from the cytosol to the nucleus

in NRK-52E cells treated with pravastatin (Fig. 5Bc). This effect was significantly decreased

in cells treated with the COX-2 inhibitor NS-398 (Fig. 5Bd).

Pravastatin-activated *HO-1* gene expression is involved in a PPARα-dependent

pathway in NRK-52E cells. To clarify whether the increase in expression of HO-1 induced

by pravastatin was dependent on translocation of PPARα, a PPRE primer was designed for

electrophoretic mobility shift assay using a PPAR-binding sequence located in the HO-1

promoter (position −621 to −500) from rat DNA. PPARα DNA-binding activity was observed

in nuclear extracts of pravastatin-treated NRK-52E cells, and this was markedly suppressed

in cells pretreated with unlabeled primer (Fig. 6A). To further examine whether the PPARα

protein was located in the nucleus and associated with PPRE, a ChIP assay was performed

with control and pravastatin-treated cells. As shown in Fig. 6B, the association of PPARα

with the PPRE region of the HO-1 promoter was increased in pravastatin-treated cells.

Finally, to determine the role of pravastatin-induced PPARα in activating PPRE and

HO-1 promoter activity, NRK-52E cells were cotransfected with increasing amounts of a

luciferase expression vector with the PPRE reporter or a 4.5-kb human HO-1

promoter-reporter construct, along with pcDNA3-retinoid X receptor (RXR) α and

pcDNA3-FLAG-PPARα or the PPARα agonist WY14643 (Cayman Chemical). As shown in

Fig. 6C, PPARα or RXRα alone slightly increased luciferase activity, but combined

transfection with PPARα and RXRα increased luciferase activity by approximately 50-fold in

cells with the PPRE reporter and approximately 6-fold in cells with the HO-1 promoter

construct. In addition, treatment with pravastatin augmented luciferase activity in both the

PPRE and HO-1 promoters compared to cells untreated with pravastatin or transfected with

PPARα or RXRα alone. Treatment with WY14643 also increased luciferase activity by

approximately 50-fold in cells with the PPRE reporter and approximately 8-fold in cells with

the HO-1 promoter. Pravastatin cotreatment further increased luciferase activity in both the

PPRE and HO-1 promoters compared to untreated cells.

Pravastatin induced HO-1 expression via a PPARα-dependent pathway in mice.

We next subjected C57/B6, H129 wild-type (PPARα$^{+/+}$), and PPARα$^{-/-}$ mice to pravastatin

injection. After injection of pravastatin for 2 days, expression of PPARα and HO-1 was

increased in renal extracts of wild-type C57/B6 (Fig. 7A; mRNA and protein) and wild-type

W129 mice (Fig. 7B; protein). However, the increase in HO-1 expression was markedly

attenuated in PPARα$^{-/-}$ mice (Fig. 7B). Another commonly used HMG-CoA reductase

inhibitor, simvastatin, had the same effect on HO-1 expression in wild-type and PPARα$^{-/-}$

mice with or without carboplatin treatment (Supplemental Fig. 6).

Discussion

In a previous study, we showed that carboplatin-induced cardiotoxicity was

characterized by marked increases in apoptosis (3- to 5-fold) and in the levels of caspase-3

and ROS in cardiomyocytes and that these effects could be ameliorated by treatment with

pravastatin (Cheng et al., 2008). In the present study, we extended this work to include the

effects of carboplatin in the kidney. Our findings of increased apoptosis and cleaved

caspase-3 in cultured kidney cells and in vivo demonstrated that carboplatin had similar

effects to those observed in the cardiac system. In addition, we showed that the levels of ROS

also increased in kidney cells exposed to carboplatin, suggesting the involvement of ROS in

carboplatin-induced apoptosis. Results of the present study indicate that pretreatment with

pravastatin markedly decreased carboplatin-induced renal tissue damage and ameliorated

renal dysfunction, consistent with the results of Li, Yang, et al. (2004), who showed that

pravastatin normalized serum creatinine levels in a rat model of chronic cyclosporine-induced

nephropathy.

The cardioprotective effects of atorvastatin have been shown to involve the

upregulation of COX-2 and increased production of PGI_2 (Birnbaum et al., 2005). When we

examined the effects of pravastatin on the expression of COX-2 and PGI_2, we found that both

were increased in response to pravastatin, suggesting that in kidney cells, pravastatin

17

stimulates overexpression of COX-2, resulting in increased PGI_2.

PGI$_2$ is known to mediate the translation of PPARα (Chen et al., 2009). In the present

study, we showed that nuclear PPARα was increased in NRK-52E renal epithelial cells in

response to treatment with pravastatin and that this increase was the result of translocation of

PPARα from the cytoplasm to the nucleus. The observation that translocation was blocked by

the addition of the COX-2 inhibitor NS-398 supports the hypothesis that the translocation

was mediated by PGI_2.

Many lines of inquiry have pointed to a prominent cytoprotective role for HO-1 in

modulating tissue responses to injury (reviewed by Sikorski et al., 2004). In a rat model of

renal ischemia-reperfusion injury, Gueler et al. (2007) showed that pretreatment with

cervistatin decreased renal damage and dysfunction after ischemia-reperfusion. These authors

found that HO-1 expression was increased after ischemia-reperfusion, that the increased

expression was significantly greater in rats pretreated with cervistatin, and that the protective

effect of statin was completely abolished by cotreatment with a competitive inhibitor of HO-1.

Grosser et al. (2004) reported that treatment of endothelial cells with statins resulted in

activation of the HO-1 promoter, along with accumulation of HO-1 transcript and protein. In

a study of vascular smooth muscles cells, Lee et al. (2004) reported that simvastatin increased

the level of HO-1 and suggested that p38 and the phosphatidylinositol-3-kinase and protein

kinase B (PI3K-Akt) pathway might be involved. Our present findings of significantly

18

increased levels of HO-1 transcript and protein in the kidneys of pravastatin-pretreated mice

after carboplatin-induced renal injury are consistent with these previous findings in rats. In

addition, we demonstrated that this effect was mediated by PGI_2 and PPARα. This was

further corroborated by our in vitro data, in which we showed that pravastatin treatment

increased expression of PGI_2, PPARα, and HO-1 in cultured renal tubule cells.

The work of Krönke et al. (2007) in human vascular cells showed that the HO-1

promoter contains a PPRE and that HO-1 is transcriptionally regulated by PPARα. We

showed PPRE-binding activity in nuclear extracts of pravastatin-treated NRK-52E cells, that

PPARα was associated with the HO-1 promoter, and that the association was stimulated by

pravastatin. Finally we showed that PPARα and RXRα increased expression of a plasmid

construct containing the HO-1 promoter and that this expression was stimulated by

pravastatin.

Our in vitro results showing inhibition of pravastatin-induced HO-1 activation by

NS-398 and PPARα siRNA further support the hypothesis that, in kidney cells, activation of

HO-1 by pravastatin involves in a PPARα-dependent pathway. Our experiments in

PPARα-knockout mice confirmed that in vivo, as in vitro, the increase in HO-1 expression

stimulated by treatment with pravastatin was, to some extent, dependent on a PPARα

pathway.

Taken together, our data support a relation between pravastatin and HO-1. Pravastatin

induces overexpression of COX-2, which upregulates PGI_2. PGI_2 then promotes the

translocation of PPARα to the nucleus, where it binds PPRE and induces the expression of

HO-1.

Because HO-1 plays a cytoprotective role in modulating the responses of many tissues

to different types of injury and pathologic states, it is not surprising that there would be

numerous complex tissue-specific inducers that lead to its increased expression. The

cardioprotective effects of atorvastatin have been shown to be mediated by the increased

production of multiple prostaglandins, including cytosolic phospholipase A_2 ($cPLA_2$), PGI_2,

and PGE_2, via upregulation of COX-2 (Birnbaum et al., 2005). Whether prostaglandins other

than PGI_2, such as PGE_2 and PGJ_2, augment PPARα translocation and activate HO-1

expression in our carboplatin-induced renal injury model will require further study. In

addition, PPARs other than PPARα can be activated by statins. For example, Yano et al.

(2007) reported that statins activate PPARγ in macrophages. We have not ruled out a role for

PPARγ in our model.

HO-1 degrades heme into CO and biliverdin, which have powerful anti-inflammatory,

antiapoptotic, and antioxidant effects. This likely accounts for the beneficial effect of

pravastatin in inhibiting carboplatin-induced nephrotoxicity. However, these heme

degradation products are also potentially injurious. Indeed, simvastatin induction of HO-1 has

been shown to be mediated by nuclear factor erythroid 2-related factor 2 (Nrf2) in Neuro 2A

cells, and its upregulation was significantly associated with increased apoptosis in that system

(Hsieh et al., 2008). The multiple pathways for induction of HO-1 may work synergistically

to optimize its expression under many different circumstances. Thus, the pathway we have

proposed is likely to be one of several, if not many, that regulates the expression of HO-1 and

one of several that mediates the pleiotropic effects of statins.

Our present data showed that carboplatin at a single high dose (100 mg/kg) induced

renal dysfunction in mice, as evidenced by elevated levels of blood urea nitrogen and

creatinine. It is important to note that these parameters of nephrotoxicity were observed at

least 5 days after administration of carboplatin; whereas the survival of mice continued to

decline until day 7. The decrease in survival produced by carboplatin in mice may be the

result of both nephrotoxicity and cardiomyopathy (Cheng et al., 2008). In addition, impaired

renal activity and suppressed renal expression of antioxidant enzymes may be involved

(Husain et al., 2004). Our present results showed that lower doses of carboplatin (50 mg/kg)

did not alter the level of blood urea nitrogen or creatinine (data not shown) or 7-day survival

in mice. Therefore, both dose and time of carboplatin exposure are probably important in

causing nephrotoxicity.

An interesting observation from the present study is that pravastatin did not completely

protect mice against carboplatin-induced nephrotoxicity (Figs. 2 and 3). Similar partial

effects of other statins, including cervistatin and atorvastatin, on renal ischemia-reperfusion

21

injury have been reported (Gueler et al., 2007; Gottman et al., 2007). Although the exact

reason for the insufficient effect of pravastatin is not clear at present, one possible

explanation involves an inhibitory activity of pravastatin on the mammalian target of

rapamycin (mTOR) pathway (Roudier et al., 2006). Therefore, increases in the mTOR

response as a consequence of pravastatin treatment may partially mask pravastatin's

beneficial effect on carboplatin-induced kidney injury. Additional studies of mTOR activity

are needed to further explore whether these mechanisms are important for the antiapoptotic

effect mediated by pravastatin in vitro and in vivo.

In the present study, we administered pravastatin to mice at a dose of 1 mg/kg. This

dose was lower than the daily therapeutic dose in humans (20–80 mg/kg/day) (McLean et al.,

2008). However, when we increased the dose to 10 mg/kg in mice subjected to carboplatin

treatment, the survival rate was significantly decreased compared to that in mice receiving

doses of 5 mg/kg or 1 mg/kg (data not shown). This result is in conflict with that of a

previous study that used pravastatin (100–150 mg/kg) to inhibit

ischemia-reperfusion–induced nephrotoxicity (Sharyo et al., 2008). It is possible that the high

dose of carboplatin used in our present study augmented the expression of inducible nitric

oxide synthase (Ikeda et al., 2001) and contributed to the greater production of oxidative

stress compared to that in the ischemia-reperfusion model. On the basis of our results, we

conclude that low doses of pravastatin have the potential to provide effective protection

against nephrotoxicity induced by carboplatin. However, higher doses must be administrated

carefully. Further clinical evaluations in humans are needed to determine whether pravastatin

would be an attractive drug for the treatment of acute renal injury.

In summary, this study presents a novel mechanism underlying the antiapoptotic action

of pravastatin, which confers protection against carboplatin-induced injury in the kidney. In

addition, our data highlight the critical role of PGI_2-mediated PPARα translocation in the

induction of *HO-1* gene expression. Thus, overexpression of PPARα, either by treatment with

pravastatin or gene delivery, may offer a viable strategy to prevent acute renal cell damage

and improve the outcome of carboplatin-induced injury in the kidney.

References

Agarwal A, Balla J, Alam J, Croatt AJ, Nath KA (1995) Induction of heme oxygenase in toxic renal injury: a protective role in cisplatin nephrotoxicity in the rat. *Kidney Int* **48**: 1298-1307.

Alberts DS (1995) Carboplatin versus cisplatin in ovarian cancer. *Semin Oncol* **22**: 88-90.

Birnbaum Y, Ye Y, Rosanio S, Tavackoli S, Hu ZY, Schwarz ER, Uretsky BF (2005) Prostaglandins mediate the cardioprotective effects of atorvastatin against ischemia-reperfusion injury. *Cardiovas Res* **65**: 345-355.

Chen HH, Chen TW, Lin H (2009) Prostacyclin-induced peroxisome proliferator-activated receptor α translocation attenuates NF-κB and TNF-α activation after renal ischemia-reperfusion injury. *Am J Physiol Renal Physiol* **July 29**: Epub ahead of print.

Cheng CF, Juan SH, Chen JJ, Chao YC, Chen HH, Lian WS, Lu CY, Chang CI, Chiu TH, Lin H (2008) Pravastatin attenuates carboplatin-induced cardiotoxicity via inhibition of oxidative stress associated apoptosis. *Apoptosis* **13**: 883-894.

Cuturi MC, Christoph F, Woo J, Iyer S, Brouard S, Heslan JM, Pignon P, Soulillou JP, Buelow R (1999) RDP1258, a new rationally designed immunosuppressive peptide, prolongs allograft survival in rats: analysis of its mechanism of action. *Mol Med* **5**: 820-832.

Ferrándiz ML, Devesa I (2008) Inducers of heme oxygenase-1. *Curr Pharm Des* **14**: 473-486.

Forman BM, Chen J, Evans RM (1997) Hypolipidemic drugs, polyunsaturated fatty acids, and eicosanoids are ligands for peroxisome proliferator-activated receptors α and δ. *Proc Nat Acad Sci U S A* **94**: 4312-4317.

Fujiwara K, Sakuragi N, Suzuki S, Yoshida N, Maehata K, Nishiya M, Koshida T, Sawai H, Aotani E, Kohno I (2003) First-line intraperitoneal carboplatin-based chemotherapy for 165 patients with epithelial ovarian carcinoma: results of long-term follow-up. *Gynecol Oncol* **90**: 637-643.

Gottmann U, Brinkkoetter PT, Hoeger S, Gutermann K, Coutinho ZM, Ruf T, Hui S, Liu Z, Schnuelle P, van der Woude FJ, Braun C, Yard BA (2007) Atorvastatin donor pretreatment prevents ischemia/reperfusion injury in renal transplantation in rats: possible role for aldose-reductase inhibition. *Transplantation* **84**: 755-762.

Grosser N, Hemmerle A, Berndt G, Erdmann K, Hinkelmann U, Schürger S, Wijayanti N, Immenschuh S, Schröder H (2004) The antioxidant defense protein heme oxygenase 1 is a novel target for statins in endothelial cells. *Free Radic Biol Med* **37**: 2064-2071.

Gueler F, Park JK, Rong S, Kirsch T, Lindschau C, Zheng W, Elger M, Fiebeler A, Fliser D, Luft FC, Haller H (2007) Statins attenuate ischemia-reperfusion injury by inducing heme oxygenase-1 in infiltrating macrophages. *Am J Pathol* **170**: 1192-1199.

Gueler F, Rong S, Park JK, Fiebeler A, Menne J, Elger M, Mueller DN, Hampich F, Dechend R, Kunter U, Luft FC, Haller H (2002) Postischemic acute renal failure is reduced by

short-term statin treatment in a rat model. *J Am Soc Nephrol* **13**: 2288-2298.

Hsieh CH, Rau CS, Hsieh MW, Chen YC, Jeng SF, Lu TH, Chen SS (2008)
Simvastatin-induced heme oxygenase-1 increases apoptosis of Neuro 2A cells in response
to glucose deprivation. *Toxicol Sci* **101**: 112-121.

Husain K, Whitworth C, Rybak LP (2004) Time response of carboplatin-induced
nephrotoxicity in rats. *Pharmacol Res* **50**: 291-300.

Ikeda U, Shimpo M, Ikeda M, Minota S, Shimada K (2001) Lipophilic statins augment
inducible nitric oxide synthase expression in cytokine-stimulated cardiac myocytes. *J
Cardiovasc Pharmacol* **38**: 69-77.

Kintzel PE (2001) Anticancer drug-induced kidney disorders. *Drug Saf* **24**: 19-38.

Krönke G, Kadl A, Ikonomu E, Blüml S, Fürnkranz A, Sarembock IJ, Bochkov VN, Exner
M, Binder BR, Leitinger N (2007) Expression of heme oxygenase-1 in human vascular
cells is regulated by peroxisome proliferator-activated receptors. *Aterioscler Thromb Vasc
Biol* **27**: 1276-1282.

Lee TS, Chang CC, Zhu Y, Shyy JY (2004) Simvastatin induces heme oxygenase-1: a novel
mechanism of vessel protection. *Circulation* **110**: 1296-1302.

Li S, Wu P, Yarlagadda P, Vadjunec NM, Proia AD, Harris RA, Portilla D (2004) PPARα
ligand protects during cisplatin-induced acute renal failure by preventing inhibition of
renal FAO and PDC activity. *Am J Physiol Renal Physiol* **286**: F572-F580.

Li C, Yang CW, Park JH, Lim SW, Sun BK, Jung JY, Kim SB, Kim YS, Kim J, Bang BK

(2004) Pravastatin treatment attenuates interstitial inflammation and fibrosis in a rat

model of chronic cyclosporine-induced nephrophathy. *Am J Physiol Renal Physiol* **286**:

F46-F57.

Lin H, Cheng CF, Hou HH, Lian WS, Chao YC, Ciou YY, Djoko B, Tsai MT, Cheng CJ,

Yang RB (2008) Disruption of guanylyl cyclase-G protects against acute renal injury. *J

Am Soc Nephrol* **19**: 339-348.

McLean DS, Ravid S, Blazing M, Gersh B, Shui A, Cannon CP (2008) Effect of statin dose

on incidence of atrial fibrillation: data from the Pravastatin or Atorvastatin Evaluation and

Infection Therapy-Thrombolysis in Myocardial Infarction 22 (PROVE IT-TIMI 22) and

Aggrastat to Zocor (A to Z) trials. *Am Heart J* **155**: 298-302.

Nath KA, Grande JP, Haggard JJ, Croatt AJ, Katusic ZS, Solovey A, Hebbel RP (2001)

Oxidative stress and induction of heme oxygenase-1 in the kidney in sickle cell disease.

Am J Pathol **158**: 893-903.

Pivot X, Cals L, Cupissol D, Guardiola E, Tchiknavorian X, Guerrier P, Merad L, Wendling

JL, Barnouin L, Savary J, Thyss A, Schneider M (2001) Phase II trial of a

paclitaxel-carboplatin combination in recurrent squamous cell carcinoma of the head and

neck. *Oncology* **60**: 66-71.

Roudier E, Mistafa O, Stenius U (2006) Statins induce mammalian target of rapamycin

27

(mTOR)-mediated inhibition of Akt signaling and sensitize p53-deficient cells to cytostatic drugs. *Mol Cancer Ther* **5**: 2706-2715.

Sharyo S, Yokota-Ikeda N, Mori M, Kumagai K, Uchida K, Ito K, Burne-Taney MJ, Rabb H, Ikeda M (2008) Provastatin improves renal ischemia-reperfusion injury by inhibiting the mevalonate pathway. *Kidney Int* **74**: 577-584.

Sikorski EM, Hock T, Hill-Kapturczak N, Agarwal A (2004) The story so far: Molecular regulation of the heme oxygenase-1 gene in renal injury. *Am J Physiol Renal Physiol* **286**: F425-F441.

Takemoto M, Liao JK (2001) Pleiotropic effects of 3-hydroxy-3-methylglutaryl coenzyme a reductase inhibitors. *Arterioscler Thromb Vas Biol* **21**: 1712-1719.

Yano M, Matsumura T, Senokuchi T, Ishii N, Murata Y, Taketa K, Motoshima H, Taguchi T, Sonoda K, Kukidome D, Takuwa Y, Kawada T, Brownlee M, Nishikawa T, Araki E (2007) Statins activate peroxisome proliferator-activated receptor γ through extracellular signal-regulated kinase 1/2 and p38 mitogen-activated protein kinase-dependent cyclooxygenase-2 expression in macrophages. *Circ Res* **100**: 1442-1451.

Figure Legends

Fig. 1. Carboplatin-induced expression of caspase-3 and apoptosis in kidney cells in vitro and in vivo. (A, B) Concentration- and time-dependent expression of caspase-3 in NRK-52E renal epithelial cells. NRK-52E cells were treated with carboplatin (50–800 μM) for 0 to 48 h, and caspase-3 expression was analyzed by immunoblotting. (C) Evaluation of caspase-3 expression in mice after treatment with carboplatin. C57/B6 mice were injected with 100 mg/kg carboplatin intraperitoneally, and cytosolic fractions of homogenized kidney were prepared at the indicated time points (1–2 days) and immunoblotted with antibody against caspase-3. (D) Carboplatin-induced apoptosis in mouse kidney. Mice were injected with 100 mg/kg carboplatin intraperitoneally for 2 days, and paraformaldehyde-fixed sections were prepared and stained with the terminal deoxynucleotidyl transferase dUTP nick end labeling (TUNEL) method. Histograms represent the numbers of TUNEL-positive cells (quantitative analysis of TUNEL-positive nuclei relative to total nuclei) in carboplatin-treated (100 mg/kg) (a) and control (b) mice from three independent experiments. Bar = 200 μm. **$p < 0.01$.

Fig. 2. Pravastatin-inhibited production of reactive oxygen species (ROS), caspase-3 expression, and apoptosis in response to carboplatin treatment. (A) Levels of ROS after treatment with carboplatin or pravastatin in vitro. NRK-52E cells were subjected to 100 μM carboplatin for 24 h with no additional treatment (c) or with a 30-min pre-exposure to 50 μM

pravastatin (d). Cells shown in (a) and (b) were subjected to saline and pravastatin treatment

alone, respectively. The intracellular ROS concentration was determined according to

dichlorodihydrofluorescein (DCF) fluorescence, as described in the Materials and Methods.

*$p < 0.05$ compared to carboplatin treatment. (B) Protein level of caspase-3 in NRK-52E cells.

*$p < 0.05$ compared to carboplatin treatment. (C) Terminal deoxynucleotidyl transferase

dUTP nick end labeling (TUNEL) staining of kidney sections from carboplatin-treated mice

(a) and pravastatin-treated mice (b). Histograms represent numbers of TUNEL-positive cells

in carboplatin-treated mice with or without pretreatment with pravastatin (n = 5 animals in

each group). Representative results of three separate experiments are shown. Bar = 200 μm.

**$p < 0.01$. (D) Expression of active caspase-3 protein in mice. Renal lysates from each

mouse were treated as indicated and probed with specific antibody against the cleaved, active

form of caspase-3. Data represent results from three independent experiments. Scanning

densitometry was used for semiquantitative analysis compared to β-actin. *$p < 0.05$ compared

to carboplatin treatment.

Fig. 3. Pravastatin decreased carboplatin-induced renal dysfunction and improved survival in

mice. (A) Cumulative survival after pravastatin treatment in carboplatin-injected mice. Mice

were injected intraperitoneally with pravastatin for 1 day before carboplatin treatment (100

mg/kg). Kaplan-Meier survival curves showed better survival in the pravastatin + carboplatin

group (~60%) compared to carboplatin treatment alone (~20%) over a 7-day period. (B)

Effect of pravastatin on renal function in mice after carboplatin treatment. Mice were injected

with pravastatin for 1 day and injected intraperitoneally with carboplatin (100 mg/kg) 2 days

later. Serum urea nitrogen and creatinine levels were measured 5 days after administration of

carboplatin. **$p < 0.01$ compared to carboplatin treatment. (C) Photomicrographs of kidneys

from carboplatin-treated mice (c) show severe renal failure, including extensive loss of brush

borders (blue arrow) and tubular necrosis (black arrow). Injection with pravastatin produced a

marked decrease in the severity of these features (d). (a and b) control mice and mice treated

with pravastatin alone, respectively. Sections were stained with hematoxylin and eosin. Bar =

200 μm.

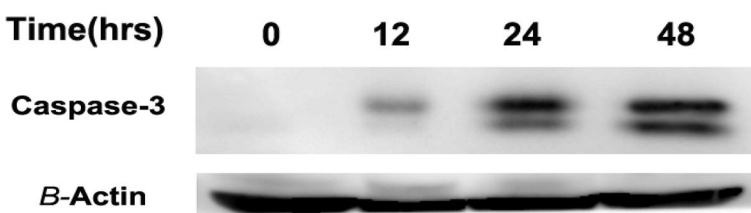**Fig. 4.** Effect of pravastatin on heme oxygenase (HO)-1 expression via a peroxisome

proliferator-activated receptor (PPAR) α–dependent pathway. (A) Pravastatin induced

expression of HO-1 and cyclooxygenase (COX)-2 in a time-dependent manner. Rat

NRK-52E renal epithelial cells were treated with 20 μM pravastatin for 24 or 48 h, and HO-1

and COX-2 levels were analyzed by immunoblotting. Representative results of three

independent experiments are shown. (B) Supernatants were assayed for PGI_2 concentration

by 6-keto prostaglandin (PG) F1α enzyme-linked immunosorbent assay. **$p < 0.01$

compared to pravastatin treatment. (C) Protein levels of PPARα and HO-1 in

pravastatin-treated cells after transfection with a plasmid encoding PPARα siRNA. *$p < 0.05$

and **$p < 0.01$ compared to pravastatin treatment. (D) Protein level of HO-1 in

pravastatin-treated cells after pretreatment with the COX-2 inhibitor NS-398 for 30 min. Cell

lysates were blotted with antibody against HO-1. Representative results from three

independent experiments are shown. Scanning densitometry was used for semiquantitative

analysis to compare against β-actin. *$p < 0.05$, **$p < 0.01$.

Fig. 5. Enhanced nuclear translocation of peroxisome proliferator-activated receptor (PPAR)

α in response to pravastatin via a PPARα-PGI$_2$–dependent pathway. (A) Translocation of

PPARα in response to pravastatin treatment. Plasmid containing FLAG-PPARα was

transfected into NRK-52E cells, and cell lysates were separated into nuclear and cytosolic

fractions and probed with specific antibody against FLAG. Representative results from two

independent experiments are shown. Scanning densitometry was used for semiquantitative

analysis to compare against β-actin. *$p < 0.05$ compared to sham treatment. (B) Subcellular

localization of FLAG-PPARα in pravastatin-treated NRK-52E cells. (a and b) In control cells

without pravastatin treatment, most of the FLAG-PPARα was located in the cytosol. (c) After

pravastatin treatment, PPARα was translocated from the cytosol to the nucleus. (d) Nuclear

translocation was decreased by pretreatment with the cyclooxygenase (COX)-2 inhibitor

NS-398. Bar = 200 μm.

Fig. 6. Pravastatin enhanced expression of heme oxygenase (HO)-1 by a peroxisome

proliferator-activated receptor (PPAR) α-PGI$_2$–dependent pathway. (A) Binding activity of

PPARα in the peroxisome proliferator response element (PPRE)-binding site of the HO-1

promoter. Results of electrophoretic mobility shift assay with the PPARα probe in nuclear

extracts of NRK-52E cells with or without treatment with pravastatin and in the presence of 0,

10×, or 100× concentration of unlabeled competitor probe. P = probe alone; C = cells alone.

(B) Chromatin was isolated from pravastatin-treated or untreated NRK-52E cells after

transfection with FLAG-PPARα plasmid. Chromatin immunoprecipitation (ChIP)

experiments were carried out with FLAG-specific antibody and primers to amplify −621

to −500 of the HO-1 locus, which contains one predicted PPAR-binding site in rats.

Immunoprecipitated DNA was quantified by quantitative polymerase chain reaction with a

TaqMan-labeled probe and normalized to the quantity of DNA in 10% of the input used for

ChIP for each sample. The data are representative of two to four independent experiments. (C)

Pravastatin induced PPRE and HO-1 promoter activity in a PPARα-dependent manner.

NRK-52E cells were transiently cotransfected with reporter construct pGL2-PPRE or pGL2

containing the HO-1-α promoter, pcDNA3.1-RXRα, or FLAG-PPARα 2 days after treatment

with or without pravastatin and/or the PPARα agonist WY14643 (200 μM) for 24 h. The

pGL2-basic plasmid served as a vector control. Cells were collected and assayed for

luciferase activity. *$p < 0.05$.

Fig. 7. Effect of pravastatin on heme oxygenase (HO)-1 expression in wild-type (peroxisome proliferator-activated receptor [PPAR] $\alpha^{+/+}$) and PPAR$\alpha^{-/-}$ mice. (A) mRNA (*top*) and protein (*bottom*) expression of PPARα and HO-1 after intraperitoneal injection of pravastatin in mice. *$p < 0.05$ compared to sham treatment. (B) Expression of HO-1 protein in wild-type (n = 5 in each group) and PPAR$\alpha^{-/-}$ mice (n = 7 in each group) with or without pravastatin treatment.

Fig.1

(A)

| | C | 50 | 100 | 200 | 400 | 800 |

Caspase-3

B-Actin

(B)

Time(hrs) 0 12 24 48

Caspase-3

B-Actin

(C)

Carboplatin — 1D 2D

Caspase-3

B-Actin

(D)

Fig.2

(A)

(B)

(C)

(D)

Fig.3

(A)

(B)

(C)

Fig.4

(A)

Time(hrs)	C	24	48

HO-1

COX-2

B-actin

(B)

6-keto PGF1α pg/μg protein

** p=0.002

Pravastatin(20μM)   —   +

(C)

PPARα

GAPDH

Nuclear extracts

HO-1

β-actin

Cytosolic extracts

Control   Pravastatin   PPARαSiRNA + Pravastatin

Relative of PPARα expression (% of GAPDH)

** p=0.004

Relative HO-1 expression level(% of β-actin)

* p=0.04

(D)

Pravastatin	—	+	—	—	+	+	+
NS398	—	—	—	+	+	—	+
PPAR-α SiRNA	—	—	+	—	—	+	+

HO-1

β-actin

Relative HO-1 expression level (% β-actin)

** p=0.004
** p=0.004
* p=0.04

Fig.5

(A)

(B)

Fig.6

(A)

(B)

(C)

Fig.7

(A)

(B)